

***R*-matrix calculation of differential cross sections for low-energy electron collisions with ground-state and electronically excited-state O₂ molecules**

Motomichi Tashiro* and Keiji Morokuma

Department of Chemistry, Emory University, 1515 Dickey Drive, Atlanta, Georgia 30322, USA

Jonathan Tennyson

Department of Physics and Astronomy, University College London, London WC1E 6BT, United Kingdom

(Received 25 April 2006; published 2 August 2006)

Differential cross sections for electron collisions with the O₂ molecule in its ground $X^3\Sigma_g^-$ state, as well as excited $a^1\Delta_g$ and $b^1\Sigma_g^+$ states are calculated. As previously, the fixed-bond *R*-matrix method based on state-averaged complete active space self-consistent-field orbitals is employed. In addition to elastic scattering of electron with the O₂ $X^3\Sigma_g^-$, $a^1\Delta_g$, and $b^1\Sigma_g^+$ states, electron impact excitation from the $X^3\Sigma_g^-$ state to the $a^1\Delta_g$ and $b^1\Sigma_g^+$ states as well as 6 eV states of $c^1\Sigma_u^-$, $A'^3\Delta_u$, and $A^3\Sigma_g^+$ states is studied. Differential cross sections for excitation to the 6 eV states have not been calculated previously. Electron impact excitation to the $b^1\Sigma_g^+$ state from the metastable $a^1\Delta_g$ state is also studied. For electron impact excitation from the O₂ $X^3\Sigma_g^-$ state to the $b^1\Sigma_g^+$ state, our results agree better with the experimental measurements than previous theoretical calculations. Our cross sections show angular behavior similar to the experimental ones for transitions from the $X^3\Sigma_g^-$ state to the 6 eV states, although the calculated cross sections are up to a factor of 2 larger at large scattering angles. For the excitation from the $a^1\Delta_g$ state to the $b^1\Sigma_g^+$ state, our results marginally agree with the experimental data except for the forward scattering direction.

DOI: 10.1103/PhysRevA.74.022706

PACS number(s): 34.80.Gs

I. INTRODUCTION

A detailed knowledge of electron collisions with the oxygen molecule is important for the physics and chemistry of both laboratory and astrophysical plasmas. In particular, recent attempts to understand the electrical discharge oxygen-iodine laser have suggested that excited electronic states of O₂ molecule play an important role [1,2]. In a previous paper [3] (henceforth denoted paper I), we studied integral cross sections for electron collisions with the O₂ molecule in its excited $a^1\Delta_g$ and $b^1\Sigma_g^+$ states, in addition to the much studied electron scattering by the O₂ $X^3\Sigma_g^-$ ground state. We used the fixed-bond *R*-matrix method with 13 target states represented by valence configuration interaction wave functions. State-averaged complete active space self-consistent-field (SA-CASSCF) orbitals with Gaussian-type basis functions were employed. The calculated cross sections for electron impact excitation from the $a^1\Delta_g$ state to the $b^1\Sigma_g^+$ state at 4.5 eV agree well with the available experimental data of Hall and Trajmar [4]. Although elastic scattering of electrons by the $a^1\Delta_g$ and $b^1\Sigma_g^+$ states was also studied, we could not find any experimental data for comparison.

In paper I, theoretical and experimental integral cross sections were compared. However, differential cross sections (DCSs) provide a more stringent test of theory and are often easier to measure reliably than integral cross sections. For electron impact electronic excitations, calculations which give good integral cross sections often give DCSs which differ significantly from those observed experimentally. In this paper, we present DCSs for the corresponding processes calculated using the same *R*-matrix model.

Previous experimental and theoretical studies in the field of electron O₂ collisions are well summarized by Brunger and Buckman [5]. Here we only review works relevant to this paper. The DCSs of electron collisions with O₂ molecule have been measured by many experimental groups. In particular, electron impact excitations to the low-lying $a^1\Delta_g$ and $b^1\Sigma_g^+$ states have been studied experimentally by Trajmar *et al.* [6], Shyn and Sweeney [7], Allan [8], Middleton *et al.* [9], and Linert *et al.* [10]. In contrast to these experimental works, only Middleton *et al.* [9] report calculations of DCSs for these excitation processes. Some of the more recent measurements have focused on electron impact excitations from the $X^3\Sigma_g^-$ ground state to the 6 eV states, i.e., the $c^1\Sigma_u^-$, $A'^3\Delta_u$, and $A^3\Sigma_g^+$ states which are also called the Herzberg pseudocontinuum [11–13]. Although these DCSs are not state resolved in most cases, Shyn and Sweeney [13] obtained cross sections for excitation to the individual electronic state within the 6 eV states. In this paper, we also calculate the DCSs of this process using the fixed-bond *R*-matrix method, since no previous theoretical calculation exists. Up to now, there is only one measurement of DCSs for electron collisions with electronically excited O₂ molecule. Hall and Trajmar [4] obtained excitation cross sections from the O₂ $a^1\Delta_g$ to the $b^1\Sigma_g^+$ state at electron impact energy of 4.5 eV. Their integral cross section was compared with our *R*-matrix results in paper I.

In this paper, details of the calculations are presented in Sec. II, and we discuss the results in Sec. III comparing our results with previous theoretical and available experiments. Then the summary is given in Sec. IV.

II. THEORETICAL METHODS

The *R*-matrix method itself has been described extensively in the literature [14–16] as well as in paper I. Thus we

*Electronic address: tashiro@euch4e.chem.emory.edu

do not repeat a general explanation of the method here. We used a modified version of the polyatomic programs in the UK molecular R -matrix codes [14] to extract T -matrix elements of the electron O_2 scatterings. These programs utilize Gaussian-type orbitals (GTO) to represent target molecule as well as a scattering electron. Although most of the past R -matrix works on electron O_2 collisions have employed Slater-type orbitals (STO), we select GTOs mainly because of the simplicity of the input and availability of basis functions. The SA-CASSCF orbitals are imported from the calculations with the MOLPRO suites of programs [17]. The use of SA-CASSCF orbitals improves the vertical excitation energies of the O_2 target states compared to the energies from HF orbitals as shown in paper I. These target orbitals are constructed from the $[5s, 3p]$ contracted basis of Dunning [18] augmented by a d function with exponent 1.8846, as in Sarpal *et al.* [19]. In the R -matrix calculations, we included 13 target states; $X^3\Sigma_g^-, a^1\Delta_g, b^1\Sigma_g^+, c^1\Sigma_g^-, A'^3\Delta_u, A^3\Sigma_u^+, B^3\Sigma_u^-, 1^1\Delta_u, f'^1\Sigma_u^+, 1^1\Pi_g, 1^3\Pi_g, 1^1\Pi_u,$ and $1^3\Pi_u$, where the last 4Π states were not included in the previous R -matrix studies performed by other groups. These target states were represented by valence configuration interaction wave functions constructed from the SA-CASSCF orbitals. In our fixed-bond R -matrix calculations, these target states are evaluated at the equilibrium bond length $R=2.3a_0$ of the $O_2 X^3\Sigma_g^-$ ground electronic state.

The radius of the R -matrix sphere was chosen to be $10a_0$ in our calculations. In order to represent the scattering elec-

tron, we included diffuse Gaussian functions up to $l=5$ with 9 functions for $l=0$, seven functions for $l=1-3$ and six functions for $l=4$ and 5. The exponents of these diffuse Gaussian were fitted using the GTOBAS program [20] in the UK R -matrix codes. Details of the fitting procedure are the same as in Faure *et al.* [20]. In addition to these continuum orbitals, we included eight extra virtual orbitals, one for each symmetry. The construction of the 17 electrons CSFs for the total system is the same as in paper I. The R -matrix calculations were performed for all eight irreducible representations of the D_{2h} symmetry, $A_g, B_{2u}, B_{3u}, B_{1g}, B_{1u}, B_{3g}, B_{2g},$ and A_u , for both doublet and quartet spin multiplicity of the electron plus target system.

The DCSs are evaluated from the T -matrix elements obtained by the R -matrix calculations. As in Gianturco and Jain [21] and Malegat [22], the DCS is expanded using the Legendre polynomials,

$$\frac{d\sigma}{d\Omega} \Big|_{ij} = \sum_k A_k P_k(\cos \theta), \quad (1)$$

where i and j denote the initial and final electronic states of the target, respectively. In exactly the same way as in Malegat [22], but for D_{2h} symmetry instead of $D_{\infty h}$ symmetry in her paper, we can derive an expression of the expansion coefficients A_k , which is

$$A_k = \sum_{l_i m_i j_i \Gamma \lambda \mu} \sum_{l'_i m'_i j'_i \Gamma' \lambda' \mu'} \frac{(-1)^{\mu+\nu} i^{l_i-l_j+l'_i+l'_j} (2k+1)}{8(2S_i+1)k_i^2} \delta_{\lambda'-\lambda, \mu'-\mu} \sqrt{(2l_i+1)(2l'_i+1)(2l_j+1)(2l'_j+1)} \\ \times \begin{pmatrix} l_i & l'_i & k \\ -\lambda & \lambda' & \lambda-\lambda' \end{pmatrix} \begin{pmatrix} l_j & l'_j & k \\ -\mu & \mu' & \mu-\mu' \end{pmatrix} \begin{pmatrix} l_i & l'_i & k \\ 0 & 0 & 0 \end{pmatrix} \begin{pmatrix} l_j & l'_j & k \\ 0 & 0 & 0 \end{pmatrix} C_{\lambda, m_i} C_{\mu, m_j}^* C_{\lambda', m'_i}^* C_{\mu', m'_j} \sum_S (2S+1) T_{il, m_i, j, l, m_j}^{\Gamma S M_S} (T_{il', m'_i, j', l', m'_j}^{\Gamma' S M_S})^*. \quad (2)$$

Details of the derivation are given in the Appendix. In Eq. (2),

$$\begin{pmatrix} l_i & l'_i & k \\ -\lambda & \lambda' & \lambda-\lambda' \end{pmatrix},$$

etc., are $3j$ coefficients, k_i is the wave number of the incident electron, S_i is the spin quantum number of the initial target state, while S is the spin quantum number of the total system and M_S is the projection of the total spin. The indices Γ and Γ' run over the eight irreducible representations of the D_{2h} point group, since we employ the polyatomic version of the UK R -matrix code. The angular quantum numbers of the scattering electron, l_i and m_i , etc., in the T -matrix element $T_{il, m_i, j, l, m_j}^{\Gamma S M_S}$ specify the real spherical harmonics S_l^m instead of the complex form Y_l^m , because the S_l^m transform as irreducible representations under D_{2h} symmetry. This means, there

are transformation matrix elements C_{λ, m_i} , etc., in the expression for A_k in order to convert the index of the scattering electron from the S_l^m representation to the Y_l^m representation. An expression of the matrix elements $C_{\lambda, m}$ is given in the Appendix. Finally, we note that the summations over $(\Gamma l_i m_i)$ should satisfy the symmetry relation, $\Gamma = \text{IR}(i) \times \text{IR}(S_l^{m_i})$, with $\text{IR}(i)$ and $\text{IR}(S_l^{m_i})$ each being an irreducible representation of the D_{2h} group corresponding to the i th target state and the real spherical harmonic $S_l^{m_i}$, respectively. This relation also holds for (Γ, l_j, m_j) , (Γ', l'_i, m'_i) , and (Γ', l'_j, m'_j) .

In Eq. (2), the T -matrix elements belonging to different total symmetries are multiplied together. Since these matrix elements come from different calculations, overall phases of molecular orbitals and target CI vectors underlying these matrix elements may be inconsistent (see Ref. [23]), which may result in erroneous relative signs of these T -matrix elements. To avoid this inconsistency, we saved reference target CI

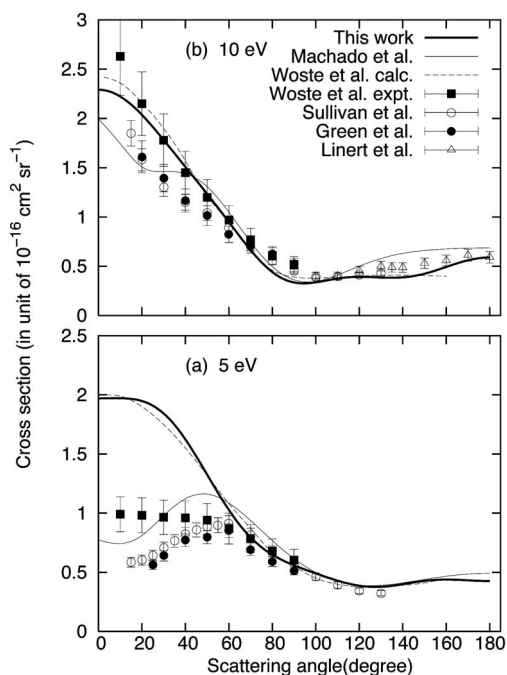


FIG. 1. Differential cross sections for elastic electron collisions with the $\text{O}_2 X^3\Sigma_g^-$ state. (a) Electron impact energy of 5 eV and (b) 10 eV. Thick full line represents our result. For comparison, previous theoretical results of Wöste *et al.* [24] and Machado *et al.* [25] are shown as thin lines. Symbols with error bars indicate experimental cross sections of Wöste *et al.* [24], Sullivan *et al.* [31], Green *et al.* [32], and Linert *et al.* [26].

vectors from the first calculation, A_g symmetry for example, and then aligned the overall phases of the target CI vectors in other calculations, B_{2u} , B_{3u} , B_{1g} , B_{1u} , B_{3g} , B_{2g} , A_u symmetries, according to this reference. The same set of molecular orbitals was used in all these calculations.

III. RESULTS AND DISCUSSION

A. Electron collisions with the $\text{O}_2 X^3\Sigma_g^-$ ground state

Figure 1 shows DCSs for elastic electron scattering from the $\text{O}_2 X^3\Sigma_g^-$ state compared with previous theoretical and experimental results. Our results are very similar to the previous *R*-matrix cross sections of Wöste *et al.* [24]. The cross sections of Machado *et al.* [25] were calculated using the Schwinger variational iterative method combined with the distorted-wave approximation. Their results at 5 eV are much lower than the *R*-matrix results at low scattering angle below 50 degrees. Our results agree reasonably well with the experimental cross sections at 10 eV, including the recent results of Linert *et al.* [26] for backward scattering. At 5 eV, our model significantly overestimates the cross sections for forward scattering compared to the experimental values. For example, our result is twice as large as the experimental values at 10° . This situation is the same in the previous *R*-matrix calculation of Wöste *et al.* [24]. As discussed by Wöste *et al.*, this deviation can be attributed to a lack of long-range polarizability in the scattering model. For example, Gillan *et al.* [27] introduced polarized pseudostates to

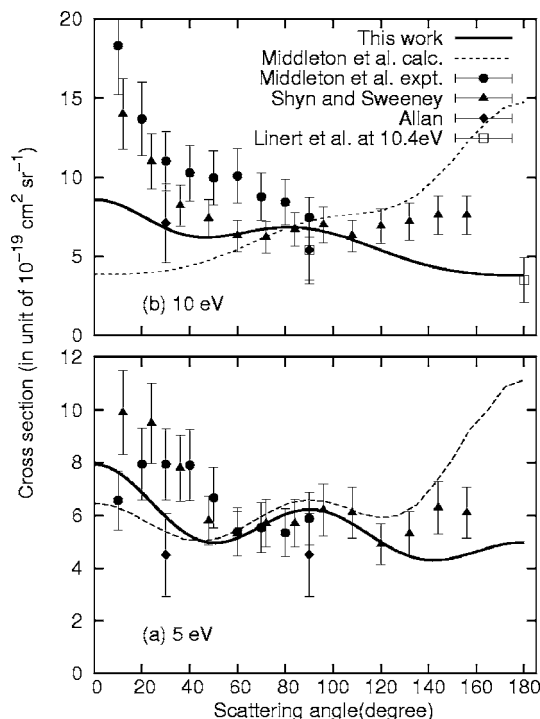


FIG. 2. Differential cross sections for electron impact excitation from the $\text{O}_2 X^3\Sigma_g^-$ state to the $a^1\Delta_g$ state. (a) Electron impact energy of 5 eV and (b) 10 eV. Full line represents our result. For comparison, we include previous theoretical and experimental cross sections of Middleton *et al.* [9], experimental results of Shyn and Sweeney [7], Allan [8] and Linert *et al.* [10].

account for the long-range polarizability in electron- N_2 scattering and reduced the cross sections by 50% in the threshold energy region. The interaction potential of Machado *et al.* [25] includes the correlation-polarization term based on the free-electron-gas model. Probably the polarization introduced by this term is responsible for their better agreement with experiment at 5 eV. Since we are interested in electron collisions with the excited electronic states of O_2 in this work, we choose not to pursue precise accuracy further for the ground state elastic scattering. However, we must be mindful that similar long-range polarizability problems may exist in the other low-energy electron scattering processes, especially elastic electron scattering of the $a^1\Delta_g$ and $b^1\Sigma_g^+$ state O_2 molecules, which will be discussed below.

The DCSs for excitation to the $a^1\Delta_g$ state at electron impact energy 5 and 10 eV are compared in Fig. 2 with the previous theoretical calculation and the experimental measurements of Middleton *et al.* [9], Shyn and Sweeney [7], Allan [8], and Linert *et al.* [10]. The cross sections at 5 eV agrees well with the previous calculation and experimental data below 120° . However, our results are much lower than the previous calculation of Middleton *et al.* at scattering angle above 130° . At an electron scattering energy of 10 eV, our cross section deviates further from the previous calculation of Middleton *et al.* [9] especially at scattering angle below 60° and above 140° . In contrast to the backward enhanced cross sections of Middleton *et al.*, our DCSs have a slightly forward enhanced character. Our results agree better with the experimental data at low scattering angles than the

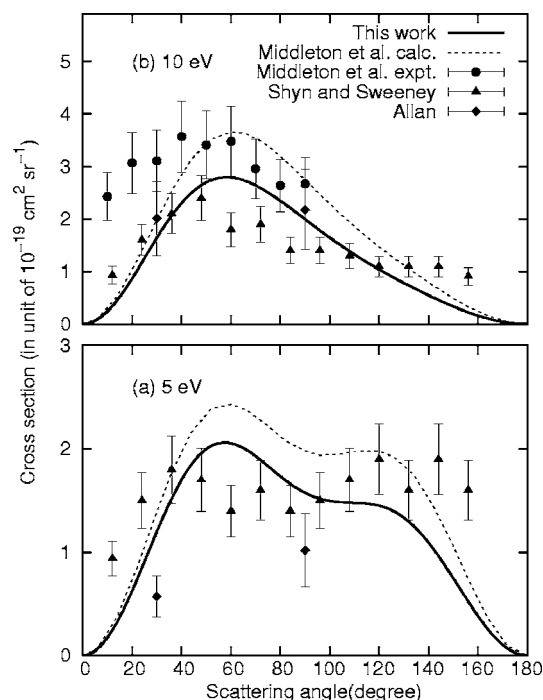


FIG. 3. Differential cross sections for electron impact excitation from the $O_2 X^3\Sigma_g^-$ state to the $b^1\Sigma_g^+$ state. Other details are the same as in Fig. 2.

previous calculation of Middleton *et al.* [9]. At large scattering angle, our results deviate from the experimental data of Shyn and Sweeney [7], but agrees rather well with the recent measurement of Linert *et al.* [10]. The *R*-matrix model of Middleton *et al.* [9] included the lowest nine O_2 target states and $l=0-5$ scattering electron orbitals with σ , π , and δ symmetry. In this work, we included 13 target states and all components of $l=0-5$ scattering electron orbitals. In addition to these differences, Middleton *et al.* used HF STO orbitals where we employed CASSCF GTO orbitals. We carried out a test calculation with $l=0-3$ scattering electron orbitals and got almost the same cross sections as in the $l=0-5$ case, which suggests that difference in the number of target states may be important for the shape of these excitation cross sections.

Figure 3 compares DCSs for excitation to the $b^1\Sigma_g^+$ state at electron impact energy of 5 and 10 eV with the previous *R*-matrix calculation and the experimental measurements of Middleton *et al.* [9], Shyn and Sweeney [7], and Allan [8]. Transitions between Σ^+ and Σ^- target states are forbidden at scattering angles of 0° and 180° , because the scattered electron wave function vanishes in the plane defined by incident electron beam and the molecular axis for any orientation of the molecule [28,29]. As a consequence, the DCSs decrease to be zero toward 0° and 180° . As is apparent from Fig. 3, our cross sections become zero at 0° and 180° , which is consistent with this selection rule. Compared to the previous *R*-matrix calculations of Middleton *et al.* [9], our cross sections have similar profile, but with slightly smaller magnitude at all scattering angles. Agreement with experiment is good at 5 eV below 120° , although our results underestimate the experimental cross sections at larger scattering angles. At

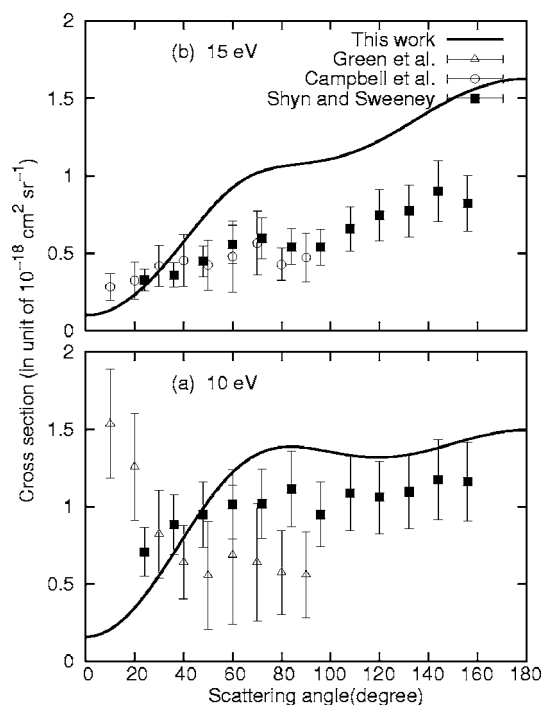


FIG. 4. Differential cross sections for excitation from the $O_2 X^3\Sigma_g^-$ state to the 6 eV states which consist of the $c^1\Sigma_u^-$, $A'^3\Delta_u$, and $A^3\Sigma_u^+$ states. The cross sections shown here are the sum of the individual cross sections of these three states. (a) Electron impact energy of 10 eV and (b) 15 eV. For comparison, we include experimental results of Green *et al.* [12], Campbell *et al.* [11], and Shyn and Sweeney [13].

10 eV, the magnitude of the experimental cross sections of Middleton *et al.* [9] and Shyn and Sweeney [7] do not agree with each other, however our cross sections are closer to the results of Shyn and Sweeney at low scattering angles below 50° . Between 60° and 90° , our results are closer to the results of Middleton *et al.*

Figure 4 shows DCSs for excitations to the 6 eV states for electron impact energies of 10 and 15 eV. Here the 6 eV states means the group of the $O_2 c^1\Sigma_u^-$, $A'^3\Delta_u$, and $A^3\Sigma_u^+$ states. The cross sections shown in Fig. 4 are a sum of individual excitation cross sections of these three electronic states, in line with most experimental measurements. The figure includes the recent experimental cross sections of Campbell *et al.* [11], Green *et al.* [12], and Shyn and Sweeney [13]. The individual cross sections are shown in Figs. 5 and 6 for impact energies of 10 and 15 eV, together with the state-resolved experimental cross sections of Shyn and Sweeney [13]. Our summed cross sections given in Fig. 4 are backward-enhanced for both the 10 and 15 eV cases, in accordance with the experimental cross sections Campbell *et al.* [11] and Shyn and Sweeney [13]. However, the forward enhancement of the DCSs at 10 eV observed by Green *et al.* [12] is not reproduced by our calculation. The individual cross sections in Figs. 5 and 6 show similar angular behavior compared to the experimental results of Shyn and Sweeney. However our DCSs for excitation to the $A'^3\Delta_u$ state is more steep toward backward direction. Also the peak in the $A^3\Sigma_u^+$ state cross sections is more pronounced in our

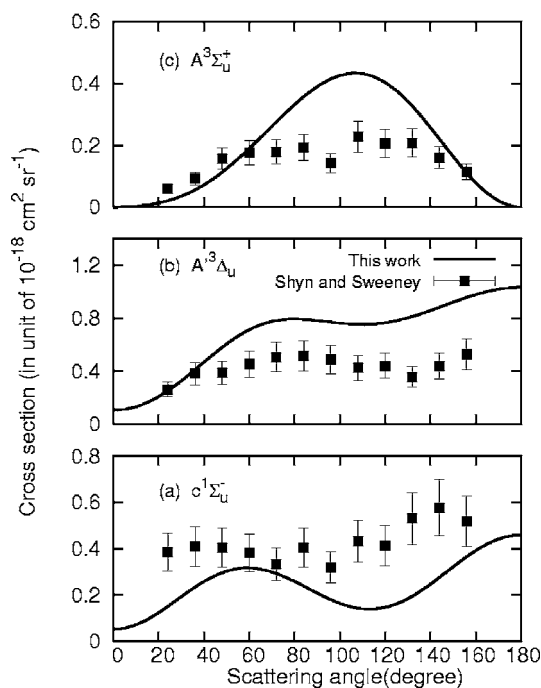


FIG. 5. Differential cross sections for excitation from the $O_2 X^3\Sigma_g^-$ state to the individual state of the 6 eV states. (a) Shows excitation cross sections for the $c^1\Sigma_u^-$ state, (b) is for the $A^3\Delta_u$ state, and (c) is for the $A^3\Sigma_u^+$ state. The electron impact energy is 10 eV. The experimental data was taken from Shyn and Sweeney [13].

calculation. Note that our results for the $A^3\Sigma_u^-$ state become zero at 0° and 180° as dictated by the $\Sigma^-\Sigma^+$ selection rule.

B. Electron collisions with the $O_2 a^1\Delta_g$ and $b^1\Sigma_u^+$ excited states

The DCSs for elastic electron scattering with the excited $O_2 a^1\Delta_g$ and $b^1\Sigma_u^+$ states are shown in Fig. 7. We cannot compare them with previous theoretical or experimental work, since there is no available data. These DCSs show strong similarity with those of the elastic electron scattering with the $X^3\Sigma_g^-$ ground state in Fig. 1. The magnitude of these cross sections is almost the same for the 10 eV case. All of them have a large forward peak at 0° , a small rise in the cross sections at 180° . The location of the minimum moves inward from 140° to 90° as the electron scattering energy increases. This similarity is also reflected in the integral cross sections for elastic electron collisions with the $X^3\Sigma_g^-$, $a^1\Delta_g$, and $b^1\Sigma_u^+$ states. The profiles and magnitudes of the integral cross sections are basically the same for all these three electronic states as shown in paper I. The main configuration of these three electronic states has the form (core) $\pi_g^4\pi_u^2$, and this may be responsible for this similarity. Our R -matrix calculations tend to overestimate the elastic scattering cross sections of the $X^3\Sigma_g^-$ state at low scattering angles, below 50° , compared to the experimental data. Considering the strong similarity of the cross section profiles for elastic scattering from excited states and the ground state, our calculations may also overestimate the cross section at low scattering angle at low electron impact energy.

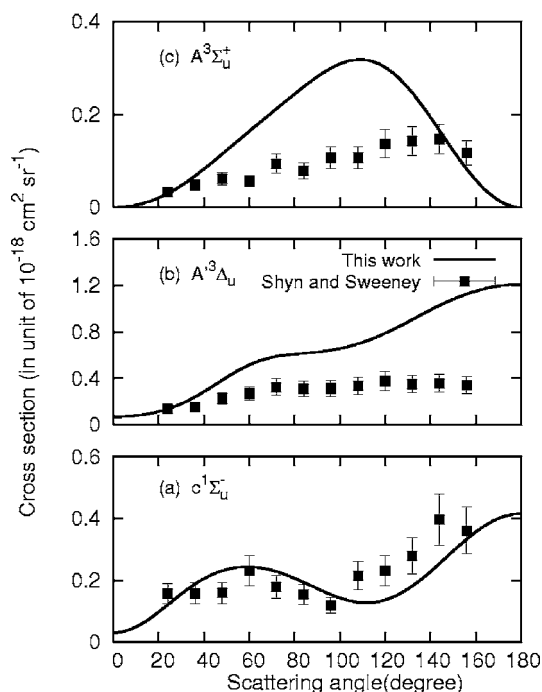


FIG. 6. The same as in Fig. 5, but for an electron impact energy of 15 eV.

In Table I, we show momentum transfer cross sections for electron elastic scattering by the $X^1\Sigma_g^-$, $a^1\Delta_g$, and $b^1\Sigma_g^+$ states. As a consequence of the similarity in DCSs, the momentum transfer cross sections have a similar magnitude. Compared to the experimental data of Shyn and Sharp [30]

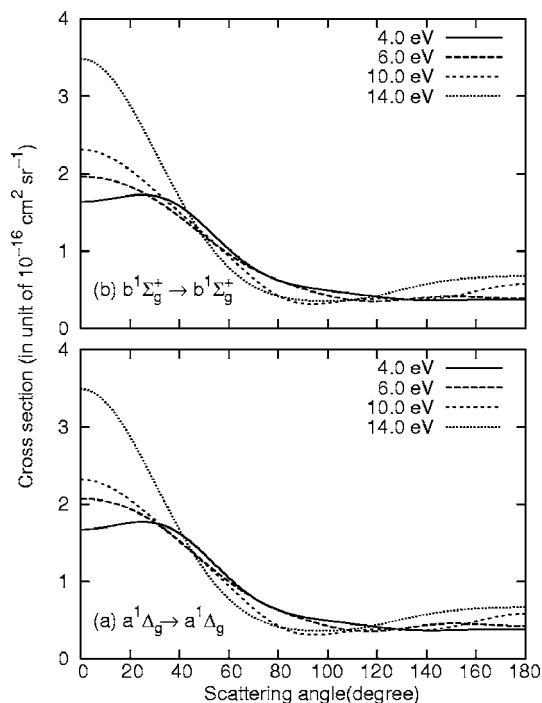


FIG. 7. Differential cross sections for elastic scattering of the O_2 excited states. (a) The $a^1\Delta_g$ state, (b) the $b^1\Sigma_g^+$ state. Each line corresponds to a different electron impact energy as shown in the legend.

TABLE I. Elastic momentum transfer cross sections in unit of 10^{-16} cm².

Electron impact energy (eV)	2.0	4.0	6.0	8.0	10.0	14.0	
This work	$X^3\Sigma_g^-$	8.18	6.80	6.73	6.06	6.04	6.96
	$a^1\Delta_g$	8.16	6.69	6.57	5.90	5.86	6.79
	$b^1\Sigma_g^+$	7.95	6.57	6.29	5.83	5.85	6.73
Shyn and Sharp [30]	$X^3\Sigma_g^-$	6.7				8.4	
Sullivan <i>et al.</i> [31]	$X^3\Sigma_g^-$	6.5	6.0		6.2	6.4	

and Sullivan *et al.* [31], our calculation overestimates the $X^3\Sigma_g^-$ state momentum transfer cross section at 2 eV by 20%, but underestimates the cross section at 10 eV by 8% of Sullivan *et al.* value or 29% of the Shyn and Sharp value. Our momentum transfer cross sections for the $a^1\Delta_g$ and $b^1\Sigma_g^+$ states may similarly be overestimates or underestimates depending on the electron impact energy.

Figure 8 shows DCSs for electron impact excitation from the $a^1\Delta_g$ state to the $b^1\Sigma_g^+$ state. The figure also includes the experimental data of Hall and Trajmar [4] at impact energy of 4.5 eV. Our cross section profiles have characteristic features of minima around 10° and 90° and maxima around 50° and 150°. They agree with the experimental cross sections of Hall and Trajmar [4] within their error bars except at 20° and 30°. The cross sections of Hall and Trajmar appear to increase from 50° to 0° whereas our cross sections decrease from 60° toward 10°. In the 50°–140° angular region, Hall and Trajmar's cross sections vary less than ours. However, a precise comparison is difficult because of large error bars and lack of other experimental data.

IV. SUMMARY

We have calculated differential cross sections for electron collisions with the O₂ molecule in its ground $X^3\Sigma_g^-$ state, as

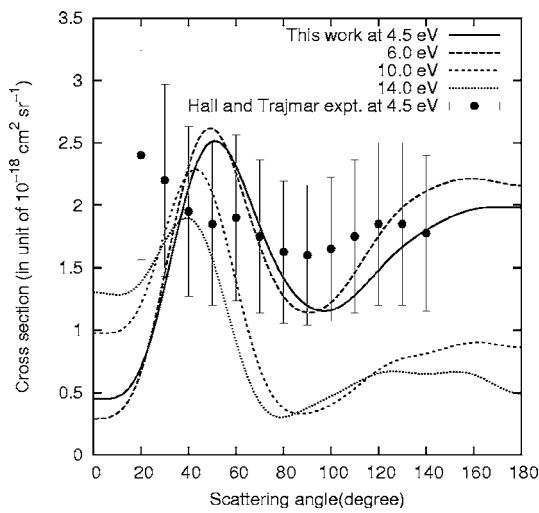


FIG. 8. Differential cross sections for electron impact excitation from the O₂ $a^1\Delta_g$ state to the $b^1\Sigma_g^+$ state. Each line corresponds to a different electron impact energy, as shown in the legend. Experimental cross sections at 4.5 eV of Hall and Trajmar [4] are also shown.

well as excited $a^1\Delta_g$ and $b^1\Sigma_g^+$ states. As in our previous work, we employed the fixed-bond *R*-matrix method based on state-averaged complete active space SCF orbitals. In addition to elastic scattering of electron with the O₂ $X^3\Sigma_g^-$, $a^1\Delta_g$ and $b^1\Sigma_g^+$ states, we studied electron impact excitations from the $X^3\Sigma_g^-$ state to the $a^1\Delta_g$ and $b^1\Sigma_g^+$ states as well as 6 eV states of $c^1\Sigma_u^-$, $A'^3\Delta_u$, and $A^3\Sigma_u^+$ states. DCSs for the excitations to the 6 eV states were not calculated previously. We also studied electron impact excitation to the $b^1\Sigma_g^+$ state from the metastable $a^1\Delta_g$ state. For electron impact excitation from the O₂ $X^3\Sigma_g^-$ state to the $b^1\Sigma_g^+$ state, our results agree better with the experimental measurements than the previous theoretical cross sections. Our cross sections show similar angular behavior to the experimental ones for transitions from the $X^3\Sigma_g^-$ state to the 6 eV states. For the excitation from the $a^1\Delta_g$ state to the $b^1\Sigma_g^+$ state, our results marginally agree with experimental data except for the forward scattering direction.

ACKNOWLEDGMENTS

The present research is supported in part by the grant from the Air Force Office of Scientific Research: the Advanced High-Energy Closed-Cycle Chemical Lasers project (PI: Wayne C. Solomon, University of Illinois, Contract No. F49620-02-1-0357). Computer resources were provided in part by the Air Force Office of Scientific Research DURIP Grant No. (FA9550-04-1-0321) as well as by the Cherry L. Emerson Center for Scientific Computation at Emory University. The work of one of the authors (M.T.) was supported by the Japan Society for the Promotion of Science Postdoctoral Fellowships for Research Abroad.

APPENDIX: DERIVATION OF EQUATION (2)

Derivation of the DCS formula in Eq. (2) is similar to that of Malegat [22] except for the use of real spherical harmonics S_l^m employed in the polyatomic version of UK molecular *R*-matrix codes instead of complex form Y_l^m . For convenience of the reader, brief derivation of the formula is given in this Appendix. In the expressions below, we follow the notation of Malegat [22].

The scattering wave function describing collision of an electron plane wave with a molecule is expressed as

$$\begin{aligned} \Psi_i(x'_1, \dots, x'_N, \sigma', \mathbf{r}) &= \Psi_i(x'_1, \dots, x'_N) \chi_{(1/2)m_{s_i}}(\sigma') e^{ik_i z} \\ &+ \sum_j \Psi_j(x'_1, \dots, x'_N) \chi_{(1/2)m_{s_j}}(\sigma') \\ &\times F_{ij}(\hat{\mathbf{r}}) e^{ik_j r} / r. \end{aligned} \quad (\text{A1})$$

Here x denotes the space and spin coordinates of the molecular electrons. The primed coordinates refer to the molecular frame with the z' axis along the molecular symmetry axis, and the unprimed coordinates to the laboratory frame with the z axis along the incident electron beam. The incident electron has wave number k_i with spin projection m_{s_i} . The index i represents quantum numbers of the electronic state of

the target molecule, Γ_i , S_i , and M_{S_i} , whereas the index I refers to (i, m_{s_i}) collectively.

In order to expand the wave function in Eq. (A1), a symmetry adapted $(N+1)$ -electron wave function is prepared as

$$\Psi_{\bar{i}l_i m_i}^{\Gamma S M} (x'_1, \dots, x'_N, \sigma', \mathbf{r}) = \sum_{\bar{j}l_j m_j} \Psi_{\bar{j}}^{S M} (x'_1, \dots, x'_N, \sigma') S_{l_j}^{m_j}(\hat{\mathbf{r}}') \times f_{\bar{i}l_i m_i, \bar{j}l_j m_j}^{\Gamma S M} (r)/r, \quad (\text{A2})$$

where Γ , S , and M stand for symmetry of the $(N+1)$ -electron system, i.e., an irreducible representation of the D_{2h} group in this work, spin quantum number and its projection to the symmetry axis. The orbital angular momentum of the scattering electron and its projection are represented by l_i and m_i . In case of $m > 0$, the real spherical harmonics S_l^m is related to the complex form of spherical harmonics Y_l^m as [33]

$$\begin{pmatrix} Y_l^m \\ Y_l^{-m} \end{pmatrix} = \frac{1}{\sqrt{2}} \begin{pmatrix} (-1)^m & (-1)^{m_i} \\ 1 & -i \end{pmatrix} \begin{pmatrix} S_l^m \\ S_l^{-m} \end{pmatrix}. \quad (\text{A3})$$

In the $m=0$ case, we only have Y_l^0 and S_l^0 and thus the matrix element is 1. Note that S_l^m behaves as an irreducible representation under D_{2h} symmetry operations, whereas Y_l^m does not. The spin coupled function in Eq. (A2) is given by

$$\Psi_{\bar{j}}^{S M} (x'_1, \dots, x'_N, \sigma') = \sum_{M_{S_j} m_{s_j}} \langle S_j M_{S_j}, \frac{1}{2} m_{s_j} | S M_S \rangle \Psi_j (x'_1, \dots, x'_N) \times \chi_{(1/2) m_{s_j}} (\sigma'), \quad (\text{A4})$$

where $\langle S_j M_{S_j}, \frac{1}{2} m_{s_j} | S M_S \rangle$ refers to the Clebsch-Gordan coefficients and \bar{i} represents Γ_i and S_i . The radial functions in Eq. (A2) are related to the S -matrix in the asymptotic region by

$$\lim_{r \rightarrow \infty} f_{\bar{i}l_i m_i, \bar{j}l_j m_j}^{\Gamma S M} (r) = \frac{1}{\sqrt{k_j}} (e^{-i[k_j r - (1/2)l_j \pi]} \delta_{\bar{i}l_i m_i, \bar{j}l_j m_j} - e^{+i[k_j r - (1/2)l_j \pi]} S_{\bar{i}l_i m_i, \bar{j}l_j m_j}^{\Gamma S M}). \quad (\text{A5})$$

Expanding Eq. (A1) in the symmetry adapted functions of Eq. (A2) gives

$$\Psi_I (x'_1, \dots, x'_N, \sigma', \mathbf{r}) = \sum_{\bar{i}l_i m_i} \sum_{\Gamma S M} a_{\bar{i}l_i m_i}^{\Gamma S M} \Psi_{\bar{i}l_i m_i}^{\Gamma S M} (x'_1, \dots, x'_N, \sigma', \mathbf{r}). \quad (\text{A6})$$

By comparing the ingoing parts on the right- and left-hand sides, we obtain the expansion coefficient

$$a_{\bar{i}l_i m_i}^{\Gamma S M} = \frac{-i^{l_i} \sqrt{4\pi(2l_i+1)}}{2i\sqrt{k_i}} \sum_{\lambda} \mathcal{D}_{0\lambda}^{l_i*} (\alpha\beta\gamma) C_{\lambda, m_i} \times \left\langle S_i M_{S_i}, \frac{1}{2} m_{s_i} | S M_S \right\rangle, \quad (\text{A7})$$

where $\mathcal{D}_{mm'}^l (\alpha\beta\gamma)$ is the rotation matrix with the Euler angles (α, β, γ) representing rotation of the laboratory frame to the molecular frame. The matrix element $C_{\lambda, m}$, defined in Eq. (A3), relates the spherical harmonics Y_l^m and S_l^m . The collision amplitude can then be obtained by equating the outgoing parts,

$$F_{IJ}(\hat{\mathbf{r}}) = \sum_{l_i m_i l_j m_j} \sum_{\Gamma S \lambda \mu \nu} \frac{\sqrt{\pi(2l_i+1)}}{\sqrt{k_i k_j}} i^{l_i - l_j + 1} \left\langle S_i M_{S_i}, \frac{1}{2} m_{s_i} | S M_S \right\rangle \times \left\langle S_j M_{S_j}, \frac{1}{2} m_{s_j} | S M_S \right\rangle \times \mathcal{D}_{0\lambda}^{l_i*} (\alpha\beta\gamma) \mathcal{D}_{\nu\mu}^{l_j} (\alpha\beta\gamma) Y_{l_j}^{\nu}(\hat{\mathbf{r}}) C_{\lambda, m_i} C_{\mu, m_j}^* T_{\bar{i}l_i m_i, \bar{j}l_j m_j}^{\Gamma S M}. \quad (\text{A8})$$

Here we use the T -matrix elements $T_{\bar{i}l_i m_i, \bar{j}l_j m_j}^{\Gamma S M}$ instead of the S -matrix.

By summing over the final states and averaging over the initial states and the molecular orientation (α, β, γ) , the differential cross section is expressed by the Legendre polynomial expansion (1) with expansion coefficients given by Eq. (2).

[1] M. Shibata, N. Nakano, and T. Makabe, *J. Appl. Phys.* **80**, 6142 (1996).
 [2] J. T. Gudmundsson, *J. Phys. D* **37**, 2073 (2004).
 [3] M. Tashiro, K. Morokuma, and J. Tennyson, *Phys. Rev. A* **73**, 052707 (2006).
 [4] R. I. Hall and S. Trajmar, *J. Phys. B* **8**, L293 (1975).
 [5] M. J. Brunger and S. J. Buckman, *Phys. Rep.* **357**, 215 (2002).
 [6] S. Trajmar, D. C. Cartwright, and W. Williams, *Phys. Rev. A* **4**, 1482 (1971).
 [7] T. W. Shyn and C. J. Sweeney, *Phys. Rev. A* **47**, 1006 (1993).
 [8] M. Allan, *J. Phys. B* **28**, 4329 (1995).
 [9] A. G. Middleton, M. J. Brunger, P. J. O. Teubner, M. W. B. Anderson, C. J. Noble, G. Wöste, K. Blum, P. G. Burke, and C. Fullerton, *J. Phys. B* **27**, 4057 (1994).
 [10] I. Linert, G. C. King, and M. Zubek, *J. Electron Spectrosc.*

Relat. Phenom. **134**, 1 (2004).

[11] L. Campbell, M. A. Green, M. J. Brunger, P. J. O. Teubner, and D. C. Cartwright, *Phys. Rev. A* **61**, 022706 (2000).
 [12] M. A. Green, T. Maddern, M. J. Brunger, L. Campbell, D. C. Cartwright, W. R. Newell, and P. J. O. Teubner, *J. Phys. B* **35**, 3793 (2002).
 [13] T. W. Shyn and C. J. Sweeney, *Phys. Rev. A* **62**, 022711 (2000).
 [14] L. A. Morgan, J. Tennyson, and C. J. Gillan, *Comput. Phys. Commun.* **114**, 120 (1998).
 [15] P. G. Burke and J. Tennyson, *Mol. Phys.* **103**, 2537 (2005).
 [16] J. D. Gorfinkiel, A. Faure, S. Taioli, C. Piccarreta, G. Halmonova, and J. Tennyson, *Eur. Phys. J. D* **35**, 231 (2005).
 [17] H.-J. Werner *et al.*, Molpro version 2002.6, a package of ab initio programs.

- [18] T. H. Dunning, *J. Chem. Phys.* **55**, 716 (1971).
- [19] B. K. Sarpal, K. Pflingst, B. M. Nestmann, and S. D. Peyerimhoff, *J. Phys. B* **29**, 857 (1996).
- [20] A. Faure, J. D. Gorfinkiel, L. A. Morgan, and J. Tennyson, *Comput. Phys. Commun.* **144**, 224 (2002).
- [21] F. A. Gianturco and A. Jain, *Phys. Rep.* **143**, 347 (1986).
- [22] L. Malegat, *Comput. Phys. Commun.* **60**, 391 (1990).
- [23] J. Tennyson, *Comput. Phys. Commun.* **100**, 26 (1997).
- [24] G. Wöste, C. J. Noble, K. Higgins, P. G. Burke, M. J. Brunger, P. J. O. Teubner, and A. G. Middleton, *J. Phys. B* **28**, 4141 (1995).
- [25] L. E. Machado, E. M. S. Ribeiro, M.-T. Lee, M. M. Fujimoto, and L. M. Brescansin, *Phys. Rev. A* **60**, 1199 (1999).
- [26] I. Linert, G. C. King, and M. Zubek, *J. Phys. B* **37**, 4681 (2004).
- [27] C. J. Gillan, C. J. Noble, and P. G. Burke, *J. Phys. B* **21**, L53 (1988).
- [28] W. A. Goddard III, D. L. Huestis, D. C. Cartwright, and S. Trajmar, *Chem. Phys. Lett.* **11**, 329 (1971).
- [29] D. C. Cartwright, S. Trajmar, W. Williams, and D. L. Huestis, *Phys. Rev. Lett.* **27**, 704 (1971).
- [30] T. W. Shyn and W. E. Sharp, *Phys. Rev. A* **26**, 1369 (1982).
- [31] J. P. Sullivan, J. Gibson, R. J. Gulley, and S. J. Buckman, *J. Phys. B* **28**, 4319 (1995).
- [32] M. A. Green, P. J. O. Teubner, B. Mojarrabi, and M. J. Brunger, *J. Phys. B* **30**, 1813 (1997).
- [33] T. Helgaker, P. Jorgensen, and J. Olsen, *Molecular Electronic-Structure Theory* (Wiley, New York, 2000), p. 210.